# Overexpression of Mitochondrial Peroxiredoxin-3 Prevents Left Ventricular Remodeling and Failure After Myocardial Infarction in Mice

Shouji Matsushima, MD; Tomomi Ide, MD, PhD; Mayumi Yamato, PhD; Hidenori Matsusaka, MD; Fumiyuki Hattori, PhD; Masaki Ikeuchi, MD; Toru Kubota, MD, PhD; Kenji Sunagawa, MD, PhD; Yasuhiro Hasegawa, PhD; Tatsuya Kurihara, PhD; Shinzo Oikawa, PhD; Shintaro Kinugawa, MD, PhD; Hiroyuki Tsutsui, MD, PhD

***Background***—Mitochondrial oxidative stress and damage play major roles in the development and progression of left ventricular (LV) remodeling and failure after myocardial infarction (MI). We hypothesized that overexpression of the mitochondrial antioxidant, peroxiredoxin-3 (Prx-3), could attenuate this deleterious process.

***Methods and Results***—We created MI in 12- to 16-week-old, male Prx-3–transgenic mice (TG+MI, n=37) and nontransgenic wild-type mice (WT+MI, n=39) by ligating the left coronary artery. Prx-3 protein levels were 1.8 times higher in the hearts from TG than WT mice, with no significant changes in other antioxidant enzymes. At 4 weeks after MI, LV thiobarbituric acid–reactive substances in the mitochondria were significantly lower in TG+MI than in WT+MI mice (mean±SEM, 1.5±0.2 vs 2.2±0.2 nmol/mg protein; n=8 each, $P<0.05$). LV cavity dilatation and dysfunction were attenuated in TG+MI compared with WT+MI mice, with no significant differences in infarct size (56±1% vs 55±1%; n=6 each, $P$=NS) and aortic pressure between groups. Mean LV end-diastolic pressures and lung weights in TG+MI mice were also larger than those in WT+sham-operated mice but smaller than those in WT+MI mice. Improvement in LV function in TG+MI mice was accompanied by a decrease in myocyte hypertrophy, interstitial fibrosis, and apoptosis in the noninfarcted LV. Mitochondrial DNA copy number and complex enzyme activities were significantly decreased in WT+MI mice, and this decrease was also ameliorated in TG+MI mice.

***Conclusions***—Overexpression of Prx-3 inhibited LV remodeling and failure after MI. Therapies designed to interfere with mitochondrial oxidative stress including the antioxidant Prx-3 might be beneficial in preventing cardiac failure. **(*Circulation*. 2006;113:1779-1786.)**

**Key Words:** antioxidants ■ free radicals ■ heart failure ■ myocardial infarction ■ remodeling

Experimental and clinical studies have demonstrated excessive generation of reactive oxygen species (ROS) in failing hearts.[1,2] Among the potential sources of ROS within the heart, mitochondrial electron transport produces superoxide anion ($\cdot O_2^-$) in this disease state.[3] Furthermore, increased ROS leads to mitochondrial DNA (mtDNA) damage and dysfunction.[4,5] Therefore, the intimate link between mitochondrial oxidative stress, mtDNA decline, and mitochondrial dysfunction plays an important role in the development and progression of left ventricular (LV) remodeling and failure that occur after myocardial infarction (MI).

## Clinical Perspective p 1786

Peroxiredoxin-3 (Prx-3) is a mitochondrial antioxidant protein and member of the Prx family that can scavenge $H_2O_2$ in cooperation with thiol and peroxynitrite.[6] In mammals, 6 distinct Prx family members have been identified (Prx-1 through -6). Among the Prxs, Prx-3 is unique because it is localized specifically within the mitochondria.[7] Furthermore, in vivo transfer of the *Prx-3* gene protected neurons against cell death induced by oxidative stress.[8] These beneficial characteristics make Prx-3 an important candidate for therapy against LV failure after MI, in which ROS production has been demonstrated to be increased within the mitochondria.[1-3] Although several previous reports showed the beneficial effects of antioxidants on heart failure,[9,10] no study has ever been performed to specifically examine the protective role of Prx-3. To address these questions, we created transgenic (TG) mice containing the rat *Prx-3* gene. Rat Prx-3–TG mice and their wild-type (WT) littermates were randomized to receive

Received August 10, 2005; revision received January 26, 2006; accepted February 2, 2006.

From the Department of Cardiovascular Medicine, Graduate School of Medical Sciences (S.M., T.I., H.M., M.I., T.K., K.S.), and the Department of Redox Medicinal Science, Graduate School of Pharmaceutical Sciences (M.Y.), Kyushu University, Fukuoka; Biomedical Research Laboratories (F.H., Y.H., T.K., S.O.), Daiichi Suntory Pharma Co, Ltd, Osaka; and the Department of Cardiovascular Medicine (S.K., H.T.), Hokkaido University Graduate School of Medicine, Sapporo, Japan.

Correspondence to Hiroyuki Tsutsui, MD, PhD, Department of Cardiovascular Medicine, Hokkaido University Graduate School of Medicine, Kita-15, Nishi-7, Kita-ku, Sapporo 060-8638, Japan. E-mail htsutsui@med.hokudai.ac.jp



*Circulation* is available at http://www.circulationaha.org

DOI: 10.1161/CIRCULATIONAHA.105.582239

either a large transmural MI induced by coronary artery ligation or sham operation.

## Methods

### Generation of TG Mice

The rat Prx-3 cDNA fragment including the entire open reading frame from nucleotide 5 to 802 was amplified by polymerase chain reaction (PCR) and cloned into pCRII (Invitrogen, Carlsbad, Calif). An expression vector for Prx-3 was constructed with pQBI25 (TaKaRa), and the gene for green fluorescent protein was removed at the site of *Nhe*I-*Bam*HI. A cytomegalovirus promoter–driven expression cassette containing rat Prx-3 cDNA in the sense orientation was purified by ultracentrifugation with CsCl. The pronuclei of fertilized eggs from hyperovulated C57BL/6J mice were randomly microinjected with this DNA construct. Tail clips and a PCR protocol to confirm the genotype were performed by one group of investigators. Homozygous TG mice and C57BL/6J WT mice were used at 12 to 16 weeks of age. The study was approved by our institutional animal research committee and conformed to the animal care guidelines of the American Physiological Society.

### Creation of MI

We created MI in 12- to 16-week-old, male TG mice (TG+MI) and nontransgenic WT littermates (WT+MI) by ligating the left coronary artery. Sham operation without coronary artery ligation was also performed in WT (WT+sham) and TG (TG+sham) mice. This assignment procedure was performed with the use of numeric codes to identify the animals.

### Prx-3 Protein

Prx-3 protein levels were analyzed in cardiac tissue homogenates by Western blot analysis with a monoclonal antibody against rat Prx-3. Our preliminary studies revealed that this antibody against rat Prx-3 cross-reacted with mouse Prx-3 as a single band of 25 kDa. In brief, the LV tissues were homogenized with lysis buffer (20 mmol/L Tris-HCl, 1 mmol/L EDTA, 1 mmol/L EGTA, and 1 mmol/L phenylmethylsulfonylfluoride; pH 7.4). After centrifugation, equal amounts of protein (5 μg protein/lane), estimated by the Bradford method with a protein assay (Bio-Rad, Hercules, Calif), were electrophoresed on a 15% sodium dodecyl sulfate–polyacrylamide gel and then electrophoretically transferred to a nitrocellulose membrane (Millipore, Billerica, Mass). After being blocked with 5% nonfat milk in phosphate-buffered saline (PBS) containing 0.05% Tween 20 at 4°C for 1 hour, the membrane was incubated with the first antibody and then with the peroxidase-linked second antibody (Amersham Pharmacia, Uppsala, Sweden). Chemiluminescence was detected with an enhanced chemiluminescence Western blot detection kit (Amersham Pharmacia) according to the manufacturer's recommendation.

To further assess the subcellular localization of Prx-3 protein, mitochondrial and cytoplasmic fractions were prepared from LVs and subjected to Western blot analysis. In brief, the LV tissues were homogenized at 4°C for 1 minute in 6 volumes of buffer consisting of 10 mmol/L HEPES-NaOH (pH 7.4), 1 mmol/L disodium EDTA, and 250 mmol/L sucrose. The homogenate was centrifuged at 4°C and 3000*g* for 10 minutes to remove any nuclear and myofibrillar debris, and the resultant supernatant was centrifuged at 10 000*g* for 10 minutes to separate any cardiac subcellular fractions. The supernatant was used for the cytoplasmic fraction assay. To isolate the mitochondrial fraction, the pellet was resuspended at 4°C in a buffer consisting of 10 mmol/L HEPES-NaOH (pH 7.4), 1 mmol/L sodium EDTA, and 250 mmol/L sucrose and was washed 3 times with the same buffer. Murine antibodies directed toward glyceraldehyde 3-phosphate dehydrogenase (GAPDH) and cytochrome oxidase (COX) subunit I were also used to verify the integrity of these subcellular fractions.

### Immunohistochemistry

Frozen sections of cardiac tissues were incubated in the presence of 100 nmol/L MitoTracker Red CMXRos (Molecular Probes, Eugene, Ore) at 37°C for 20 minutes. We did not repeat the freeze/thaw procedure to avoid the loss of mitochondrial integrity. After being washed with PBS (10 mmol/L sodium phosphate, pH 7.4, and 150 mmol/L NaCl), the sections were fixed with 3.7% formaldehyde for 5 minutes. After being washed, the fixed sections were incubated with 100-fold–diluted anti-rat Prx-3 antibody (10 μg/mL) in PBS at 4°C overnight. Fluorescence images were taken with a confocal laser scanning microscope (Bio-Rad MRC 1024) with laser beams of 488 and 568 nm for excitation.

### Myocardial Antioxidant Enzyme Activities and Lipid Peroxidation

For the subsequent biochemical studies, the myocardial tissues with MI were carefully dissected into 3 parts: one consisting of the infarcted LV, one consisting of the border zone LV with the peri-infarct rim (a 1-mm rim of normal-appearing tissue), and one consisting of the remaining noninfarcted (remote) LV. The antioxidant enzymatic activities of superoxide dismutase (SOD), catalase, and glutathione peroxidase (GSHPx) were measured in the noninfarcted LV.[11] The formation of lipid peroxides was measured in the mitochondrial fraction isolated from the LV myocardium with use of a biochemical assay with thiobarbituric acid–reactive substances (TBARS).[4]

### Survival

A survival analysis was performed in WT+sham (n=15), TG+sham (n=14), WT+MI (n=39), and TG+MI (n=37) mice. During the study period of 4 weeks, the cages were inspected daily for deceased animals. All deceased mice were examined for the presence of MI as well as pleural effusion and cardiac rupture.

### Echocardiographic and Hemodynamic Measurements

At 4 weeks after surgery, echocardiographic studies were performed under light anesthesia with tribromoethanol/amylene hydrate (2.5% wt/vol, 8 μL/g IP) and spontaneous respiration. Two-dimensional, targeted M-mode tracings were recorded at a paper speed of 50 mm/s. Under the same anesthesia with Avertin, a 1.4F micromanometer-tipped catheter (Millar Instruments, Houston, Tex) was inserted into the right carotid artery and then advanced into the LV to measure LV pressures. One subset of investigators who were not informed of the experimental group assignments performed the in vivo LV function studies.

### Infarct Size

To measure infarct size 28 days after MI, the heart was excised and the LVs were cut from apex to base into 3 transverse sections. Five-micron sections were cut and stained with Masson's trichrome. Infarct length was measured along the endocardial and epicardial surfaces in each of the cardiac sections, and the values from all specimens were summed. Infarct size (as a percentage) was calculated as total infarct circumference divided by total cardiac circumference.[12]

In addition, to measure infarct size after 24 hours (when most animals were still alive), a separate group of animals including WT+MI (n=5) and TG+MI (n=5) mice was created by ligating the left coronary artery according to the same methods described earlier. After 24 hours of coronary artery ligation, Evans blue dye (1%) was perfused into the aorta and coronary arteries, and tissue sections were weighed and then incubated with a 1.5% triphenyltetrazolium chloride solution. The infarct area (pale), the area at risk (not blue), and the total LV area from each section were measured.[13] In our preliminary study, we confirmed excellent reliability of infarct size measurements, in which a morphometric method similar to that performed in this study was used. The intraobserver and interob-

server variabilities between 2 measurements divided by these means, expressed as a percentage, were each <5%.

### Myocardial Histopathology and Apoptosis

Myocyte cross-sectional area and collagen volume fraction were determined by quantitative morphometry of tissue sections from the mid-LV. To detect apoptosis, tissue sections from the mid-LV were stained with terminal deoxynucleotidyl transferase–mediated dUTP nick end-labeling (TUNEL) staining. The number of TUNEL-positive cardiac myocyte nuclei was counted, and the data were normalized per $10^5$ total nuclei identified by hematoxylin-positive staining in the same sections. The proportion of apoptotic cells was counted in the noninfarcted LV. We further examined whether apoptosis was present by the more sensitive ligation-mediated PCR fragmentation assays (Maxim Biotech, Inc, Rockville, Md).

### mtDNA Copy Number

DNA was extracted from cardiac tissues, and a Southern blot analysis was performed to measure the mtDNA copy number, as described earlier.[4] Primers for the mtDNA probe corresponded to nucleotides 2424 to 3605 of the mouse mitochondrial genome, and those for the nuclear-encoded mouse 18S rRNA probe corresponded to nucleotides 435 to 1951 of the human 18S rRNA genome. The mtDNA levels were normalized to the abundance of the 18S rRNA gene run on the same gel.

### Mitochondrial Complex Enzyme Activity

The specific activity of mitochondrial electron transport chain complex I (rotenone-sensitive NADH-ubiquinone oxidoreductase), complex II (succinate-ubiquinone oxidoreductase), complex III (ubiquinol–cytochrome *c* oxidoreductase), and complex IV (cytochrome *c* oxidase) was measured in myocardial tissues according to methods described previously.[4] All enzymatic activities were expressed as nanomoles per minute per milligram protein.

### Plasma TBARS

The formation of TBARS in peripheral blood samples from WT+MI and TG+MI mice was measured by a fluorometric assay, as described previously.[14] In brief, 100 μL of whole blood was mixed with 1 mL of saline and centrifuged at 3000*g* for 15 minutes. The supernatant was mixed with ½N $H_2SO_4$ and 10% phosphotungstic acid, and the mixture was centrifuged. The sediment was suspended in distilled water, 0.3% thiobarbituric acid, and 0.1% butylated hydroxytoluene. The reaction mixture was then heated at 100°C for 60 minutes in an oil bath. After being cooled with tap water, the mixture was extracted with *n*-butanol and centrifuged at 1600*g* for 15 minutes. The fluorescence intensity of the organic phase was measured by spectrofluorometry with a wavelength of 510-nm excitation and 550-nm emission. Malondialdehyde standards (Sigma-Aldrich, St. Louis, Mo) were included with each assay batch, and plasma TBARS were expressed as micromoles per gram of plasma protein in reference to these standards.

### Statistical Analysis

Data are expressed as mean±SEM. Survival analysis was performed by the Kaplan-Meier method, and between-group differences in survival were tested by the log-rank test. A between-group comparison of means was performed by 1-way ANOVA, followed by *t* tests. The Bonferroni correction was applied for multiple comparisons of means. $P<0.05$ was considered statistically significant.

The authors had full access to the data and take full responsibility for their integrity. All authors have read and agreed to the manuscript as written.

## Results

We investigated 4 groups of mice, WT+sham (n=15), TG+sham (n=14), WT+MI (n=39), and TG+MI (n=37), in the present study. A survival analysis was performed for all of these mice. Subsequent echocardiographic and hemodynamic measurements were performed in the 4-week survivors: 15 WT+sham, 14 TG+sham, 25 WT+MI, and 31 TG+MI mice. These measurements could not be accomplished in 4 WT+MI and 5 TG+MI mice owing to technical difficulties. Survivor mice were further divided into 2 groups: those studied for subsequent histological analysis, including infarct size, myocyte size, and collagen volume fraction measurements as well as TUNEL staining (5 WT+sham, 5 TG+sham, 8 WT+MI, and 8 TG+MI), and those for the biochemical assay, including antioxidant enzyme activity, Prx-3 protein levels, mitochondrial lipid peroxidation, mtDNA copy number, and mitochondrial complex enzyme activities (8 WT+sham, 8 TG+sham, 8 WT+MI, and 8 TG+MI). Infarct size was not measured in the mice that died.

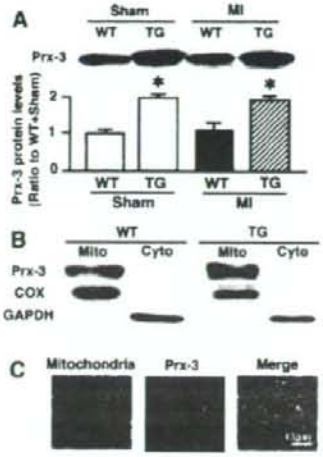


**Figure 1.** A, Representative Western blot analysis of Prx-3 protein levels (upper panels) and summary data (lower panels) in hearts from WT+sham, TG+sham, WT+MI, and TG+MI mice (n=6 each). Total protein extracts from the hearts were probed with a monoclonal antibody against rat Prx-3. The antibody recognized both rat and mouse Prx-3 as a single band of 25k Da. Data were obtained by densitometric quantification of the Western blots. Values are expressed as the ratio to the WT+sham value and mean±SEM. *$P<0.05$ for the difference from the ratio to WT+sham values. B, Localization of Prx-3 to mitochondria (mito). Western blot analysis of mitochondrial and cytoplasmic (cyto) fractions that were probed with antibodies directed toward Prx-3 as well as specific mitochondrial and cytoplasmic markers: GAPDH was detected in the cytoplasmic but not the mitochondrial fraction, and COX subunit I was detected in the mitochondrial but not the cytoplasmic fraction. Importantly, Prx-3 proteins were detected only in the mitochondrial fraction but not in the cytoplasmic fraction. C, Myocardial tissue sections from TG mice were doubly stained with MitoTracker dye (red) and a rat Prx-3–specific antibody (green). Immunoreactivity for Prx-3 was observed in the cytoplasm of cardiac myocytes. The merged images show that Prx-3 colocalized with the mitochondria (yellow). Scale bar=10 μm.

### Myocardial Antioxidants and TBARS

First, baseline differences in Prx-3 proteins as well as other antioxidant enzyme activities between WT and TG mice were determined. In TG+sham, there was a significant increase in Prx-3 protein levels in the LV compared with that of WT+sham (Figure 1A). Importantly, the antioxidants, in-

**TABLE 1. Characteristics of Animal Models**

| | WT+Sham | TG+Sham | WT+MI | TG+MI |
|---|---|---|---|---|
| Antioxidant enzymes | | | | |
| n | 7 | 7 | 7 | 7 |
| SOD, U/mg protein | 26.4±1.1 | 27.8±1.4 | 25.1±1.7 | 23.9±1.2 |
| GSHPx, nmol/min per mg protein | 74.1±3.2 | 77.7±6.7 | 87.8±4.8 | 86.1±4.2 |
| Catalase, nmol/mg protein | 79.9±6.4 | 85.0±6.2 | 87.1±3.5 | 81.4±5.8 |
| Echocardiographic data | | | | |
| n | 15 | 14 | 21 | 26 |
| Heart rate, bpm | 481±11 | 451±8 | 463±13 | 458±8 |
| LVEDD, mm | 3.47±0.05 | 3.37±0.08 | 5.51±0.13† | 4.9±0.10†§ |
| LVESD, mm | 2.22±0.05 | 2.12±0.10 | 4.78±0.13† | 4.08±0.10†§ |
| Fractional shortening, % | 35.3±0.8 | 37.0±1.1 | 13.1±0.6† | 16.9±0.6†§ |
| Hemodynamic data | | | | |
| n | 15 | 14 | 21 | 26 |
| Heart rate, bpm | 447±14 | 455±14 | 453±9 | 466±7 |
| Mean aortic pressure, mm Hg | 83±3 | 78±2 | 76±2 | 77±3 |
| LVEDP, mm Hg | 2.7±0.5 | 2.5±0.3 | 11.4±1.5† | 7.6±1.0*‡ |
| Organ weight data | | | | |
| n | 15 | 14 | 21 | 26 |
| Body wt, g | 26.9±0.5 | 27.0±0.8 | 27.0±0.3 | 26.4±0.4 |
| LV wt/body wt, mg/g | 3.2±0.1 | 3.0±0.1 | 4.6±0.3† | 4.4±0.1† |
| Lung wt/body wt, mg/g | 5.0±0.1 | 5.2±0.1 | 7.6±0.5† | 6.4±0.3†‡ |
| Pleural effusion, % | 0 | 0 | 43 | 15‡ |

EDD indicates end-diastolic diameter; ESD, end-systolic diameter; and wt, weight. Values are mean±SEM.

*$P$<0.05, †$P$<0.01 vs WT+Sham. ‡$P$<0.05, §$P$<0.01 vs WT+MI.

cluding SOD, GSHPx, and catalase activities, were not altered in the TG hearts (Table 1), indicating no effects of Prx-3 overexpression on other antioxidant enzymes. Second, the changes in antioxidants after MI were assessed. Prx-3 protein levels were significantly higher in TG+MI than in WT+MI (Figure 1A) mice. The activities of other antioxidant enzymes were not altered in WT+MI or TG+MI compared with WT+sham animals (Table 1).

The cytoplasmic marker GAPDH was detected exclusively in the cytoplasmic but not in the mitochondrial fraction, whereas COX subunit I was detected preferentially in the mitochondrial but not in the cytoplasmic fraction. This substantiates the integrity of our cellular fractions. Importantly, Prx-3 was detected only in the mitochondrial fraction but not in the cytoplasmic fraction, further confirming that Prx-3 was localized exclusively in the mitochondria (Figure 1B). In addition, immunohistochemical studies showed a homogeneous Prx-3 distribution in cardiac myocytes that colocalized with the mouse mitochondria (Figure 1C). Prx-3 staining showed a relatively spotty pattern. These results further confirm that the rat Prx-3 transgene is not expressed in the cytoplasm within the mouse heart. Mitochondrial TBARS measured in the noninfarcted LV were significantly greater in WT+MI compared with sham animals and were significantly lower in the TG+MI group (Figure 2).

## Survival

There were no deaths in the sham-operated groups. Early operative mortality (within 6 hours) was comparable between WT+MI and TG+MI animals (15% versus 7%; $P$=NS). The survival rate up to 4 weeks tended to be higher in TG+MI compared with WT+MI mice, but this difference did not reach statistical significance ($P$=0.06 by log-rank test; Figure 3A). Death was suspected to be attributable to heart failure and/or arrhythmia. Five WT+MI (15%) and 2 TG+MI (5%) mice died of LV rupture ($P$=NS).

## Infarct Size

Infarct size as determined by morphometric analysis 28 days after MI was comparable (55±1% versus 56±1%; $P$=0.83) between WT+MI (n=6) and TG+MI (n=6) groups. To further confirm that overexpression of Prx-3 did not alter infarct size, both the area at risk and infarct area were

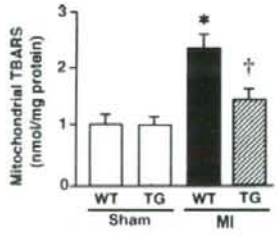


**Figure 2.** Mitochondrial TBARS in 4 experimental groups of animals (n=8 each). Values are mean±SEM. *$P$<0.05 for difference from the WT+sham value. †$P$<0.05 for difference from the WT+MI value.

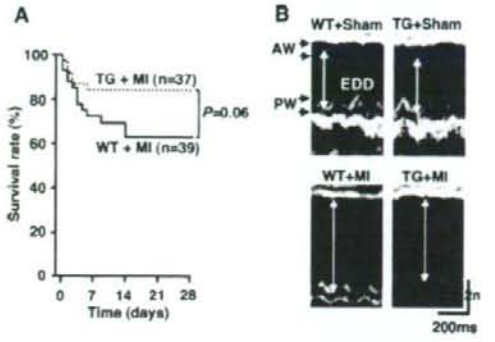


**Figure 3.** A, Kaplan-Meier survival analysis. Percentages of surviving WT+MI (n=39) and TG+MI (n=37) mice were plotted. Between-group difference was tested by the log-rank test. B, M-mode echocardiograms obtained from WT+sham, TG+sham, WT+MI, and TG+MI mice. AW indicates anterior wall; PW, posterior wall; and EDD, end-diastolic diameter.

measured in mice 24 hours after coronary artery ligation. Percentages of the LV at risk (risk area/LV, 51±3% versus 52±2%; $P=0.89$) and infarct size (infarct/risk area, 79±1% versus 78±1%; $P=0.13$) were also comparable between WT+MI (n=5) and TG+MI (n=5) animals.

### Echocardiography and Hemodynamics

The echocardiographic and hemodynamic data of surviving mice at 28 days are shown in Figure 3B and Table 1. LV diameters were significantly larger in WT+MI mice with respect to WT+sham animals. TG+MI mice displayed less LV cavity dilatation and greater fractional shortening than did WT+MI mice. There was no significant difference in heart rate or aortic blood pressure among the 4 groups of mice. LV end-diastolic pressure (LVEDP) was higher in WT+MI than in WT+sham animals, but this increase was significantly attenuated in TG+MI mice.

### Organ Weights and Histomorphometry

Coincident with an increased LVEDP, lung weight/body weight was larger in WT+MI mice, and this increase was attenuated in TG+MI mice (Table 1). The prevalence of pleural effusion was also lower in TG+MI than in WT+MI groups. Histomorphometric analysis of noninfarcted LV sections showed that myocyte cross-sectional area was greater in WT+MI mice but was significantly attenuated in TG+MI mice (Figure 4). Collagen volume fraction was greater in WT+MI mice, but this change was inhibited in TG+MI mice (Figure 4).

### Myocardial Apoptosis

There were rare TUNEL-positive nuclei in sham-operated mice. The number of TUNEL-positive myocytes in the noninfarcted LV was larger in WT+MI mice but was significantly smaller in TG+MI animals (Figure 5A). In addition, the intensity of the DNA ladder indicated that apoptosis in TG+MI animals was decreased compared with that in WT+MI mice (Figure 5B).

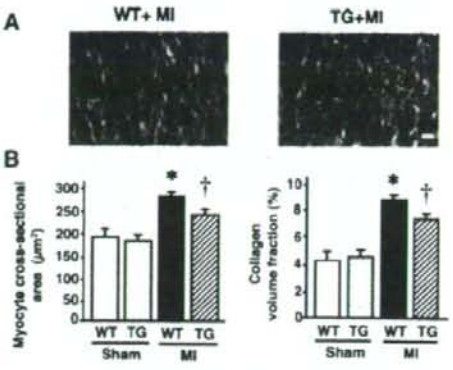


**Figure 4.** A, Photomicrographs of Masson trichrome–stained LV cross sections obtained from WT+MI and TG+MI mice. Scale bar=10 μm. B, Myocyte cross-sectional area and collagen volume fraction in WT+sham (n=5), TG+sham (n=5), WT+MI (n=8), and TG+MI (n=8) mice. Values are mean±SEM. *$P<0.05$ for difference from the WT+sham value. †$P<0.05$ for difference from the WT+MI value.

### mtDNA and Mitochondrial Complex Enzymes Activity

Consistent with our previous studies,[4] mtDNA copy number in the noninfarcted LV from WT+MI animals showed a 36% decrease ($P<0.05$) compared with that in sham-operated mice, which was significantly prevented and was preserved at normal levels in TG+MI animals (Figure 6).

To determine the effects of mtDNA alterations on mitochondrial function, we next measured the mitochondrial electron transport chain complex enzyme activities. The enzymatic activities of complexes I, III, and IV were significantly lower in the noninfarcted LV from WT+MI than in those from WT+sham animals (Table 2). Most important, no such decrease was observed in TG+MI mice. The enzymatic activity of complex II, exclusively encoded by nuclear DNA, was not altered in either group. These results indicate that mtDNA copy number and mitochondrial complex enzymatic activities are downregulated in the post-MI heart and that Prx-3 gene overexpression efficiently counteracts these mitochondrial deficiencies.

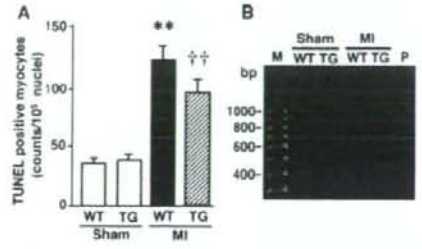


**Figure 5.** A, Numbers of TUNEL-positive myocytes in the noninfarcted LV from WT+sham, TG+sham, WT+MI, and TG+MI mice (n=5 each). Values are mean±SEM. **$P<0.01$ for the difference from the WT+sham value. ††$P<0.01$ for the difference from the WT+MI value. B, DNA ladder indicative of apoptosis in the genomic DNA from the LV. M indicates marker; P, positive control.

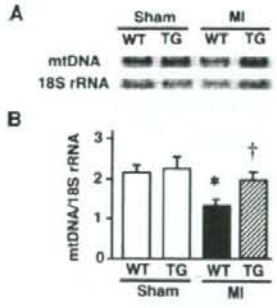


**Figure 6.** A, Southern blot analysis of mtDNA copy number in total DNA extracts from the hearts from WT+sham, TG+sham, WT+MI, and TG+MI mice. Top bands show signals from the mtDNA fragments, and bottom bands show signals from the nuclear DNA fragments containing the 18S rRNA gene. B, Summary data for a Southern blot analysis of mtDNA copy number in 4 groups of animals (n=8 each). Data were obtained by densitometric quantification of the Southern blots, such as shown in A. Values are expressed as the ratio to WT+sham values and mean±SEM. *$P<0.05$ for the difference from the WT+sham value. †$P<0.05$ for the difference from the WT+MI value.

### Plasma TBARS

Plasma TBARS were comparable between WT+MI and TG+MI mice (0.46±0.04 versus 0.54±0.05 μmol/g protein; $P$=NS).

## Discussion

The present study provides the first direct evidence that overexpression of mitochondrial antioxidant Prx-3 protects the heart against post-MI remodeling and failure in mice. It reduced LV cavity dilatation and dysfunction, as well as myocyte hypertrophy, interstitial fibrosis, and apoptosis of the noninfarcted myocardium. These beneficial effects of *Prx-3* gene overexpression were associated with an attenuation of mitochondrial oxidative stress, mtDNA decline, and dysfunction. They were not due to its MI size-sparing effect but occurred secondary to more adaptive remodeling.

Mitochondria are the predominant source of ROS in the failing myocardium.[1] Most of the $\cdot O_2^-$ generated by the mitochondria is vectorially released into the mitochondrial matrix. $\cdot O_2^-$ impairs mitochondrial function by oxidizing the Fe-S centers of complex enzymes. In addition, $\cdot O_2^-$ is converted to peroxynitrite, an extremely powerful oxidant, as a result of its reaction with NO produced by mitochondrial NO synthase. $\cdot O_2^-$ is also converted to $H_2O_2$ by a specific intramitochondrial Mn-SOD. Although Mn-SOD relieves mitochondrial oxidative stress caused by $\cdot O_2^-$, it generates $H_2O_2$ and therefore, further enhances a different type of oxidative stress. $H_2O_2$ can damage cellular macromolecules such as proteins, lipids, and nucleic acids, especially after its conversion to ·OH. Moreover, these increased ROS in the mitochondria were associated with a decreased mtDNA copy number and reduced oxidative capacity owing to low complex enzyme activities.[4] Therefore, chronic increases in mitochondrial ROS production cause mtDNA damage and dysfunction, which thus, can lead to a catastrophic cycle of further oxidative stress and ultimate cellular injury.[5] This deleterious process may play an important role in the development and progression of myocardial remodeling and failure.[4] Based on these results, mitochondrial antioxidants are expected to be the first line-of-defense mechanism against ROS generation in the mitochondria and ROS-mediated mitochondrial injury and thus, may protect the heart from adverse remodeling and failure.

Prx-3, which was formerly known as SP-22, or MER5, is currently identified as a mitochondrial member of the novel antioxidant proteins designated as Prxs.[15] Among 6 known mammalian Prxs, Prx-1 to -4 require the small redox protein thioredoxin (Trx) as an electron donor to remove $H_2O_2$, whereas Prx-5 and -6 can use other cellular reductants, such as GSH, as their electron donor.[16] Prx-1, -2, and -6 are found in the cytoplasm and nucleus,[7] whereas Prx-3 contains a mitochondrial localization sequence, is found exclusively in the mitochondria, and uses mitochondrial Trx-2 as the electron donor for its peroxidase activity.[17] It functions not only by removing $H_2O_2$ formed after the SOD-catalyzed dismutation reaction but also by detoxifying peroxynitrite.[6] Therefore, the great efficiency of Prx-3 as an antioxidant shown in the present study may be attributable to the fact that it is located in the mitochondria and can utilize lipid peroxides as well as $H_2O_2$ for substrates. In fact, overexpression of Prx-3 has been shown to protect thymoma cells from apoptosis induced by hypoxia, a bolus of peroxide, or an anticancer drug.[18] Moreover, Prx-3 overexpression has been reported to protect rat hippocampal neurons from excitotoxic injury.[8] Prx-5 is also associated with the mitochondria in addition to the peroxisomes and nucleus. Recently, increased expression of Prx-5 was found to have protected Chinese hamster ovary cells from mtDNA damage induced by oxidative stress.[19] Therefore, Prx-5 may also exert beneficial effects against mitochondrial oxidative stress in post-MI hearts.

GSHPx also catalyzes the reduction of $H_2O_2$. In fact, our previous studies demonstrated that overexpression of GSHPx

**TABLE 2. Mitochondrial Complex Enzyme Activities**

| | WT+Sham | TG+Sham | WT+MI | TG+MI |
|---|---|---|---|---|
| n | 7 | 7 | 7 | 7 |
| Complex I, nmol/min per mg protein | 282±26 | 265±38 | 159±25* | 287±16† |
| Complex II, nmol/min per mg protein | 770±70 | 718±93 | 711±85 | 726±128 |
| Complex III, nmol/min per mg protein | 505±11 | 470±31 | 367±20* | 451±21† |
| Complex IV, nmol/min per mg protein | 1223±37 | 1175±34 | 744±68* | 939±54† |

Values are mean±SEM.
*$P<0.05$ vs WT+sham; †$P<0.05$ vs WT+MI.

inhibited LV remodeling and failure after MI.[13] However, GSHPx is located predominantly in the cytosol, and only a small proportion (≈10%) is present in the mitochondria.[20] Therefore, it remains unclear whether the beneficial effects of GSHPx overexpression on post-MI hearts were attributable to an increase of this enzyme in the cytosol, the mitochondria, or both. The specific localization of Prx-3 in the mitochondria suggests that mitochondrial oxidative stress plays an important role in the development and progression of heart failure, and antioxidants localized specifically within the mitochondria provide a primary line of defense against this disease process.

A growing body of evidence suggests that ROS play a major role in the pathogenesis of cardiac failure. Furthermore, antioxidants have been shown to exert protective and beneficial effects against heart failure.[21,22] A previous study from our laboratory demonstrated that dimethylthiourea improved survival and prevented LV remodeling and failure after MI.[10] However, the most effective way to evaluate the contribution of any specific antioxidant and obtain direct evidence of an adverse role for ROS in heart failure is through gene manipulation. Therefore, the present study not only extends the previous observation that used antioxidants but also reveals the major role of mitochondrial oxidative stress in the pathophysiology of post-MI remodeling and failure.

The beneficial effects of Prx-3 overexpression shown in the present study were not due to its MI size-sparing effect, because there was no statistically significant difference in infarct size between WT+MI and TG+MI mice. Furthermore, its effects were not attributable to hemodynamics because blood pressures and heart rates were not altered (Table 1). Importantly, it is also unlikely that these effects were caused by the altered expression of antioxidant enzymes other than Prx-3 (Table 1). Moreover, the beneficial effects of Prx-3 overexpression were not due to systemic induction of antioxidant defenses. This possibility is less likely because plasma TBARS were comparable between WT+MI and TG+MI mice. Nevertheless, we cannot completely exclude the possibility that the systemic effects of Prx-3 induction might also have contributed to this phenotype because this TG is not heart-specific.

There may be several factors contributing to the protective effects conferred by Prx-3 overexpression on post-MI remodeling and failure. First, recent studies have demonstrated that a Trx-related antioxidant system is closely associated with the regulation of apoptosis, probably through quenching of ROS and redox control of the mitochondrial permeability transition pores that release cytochrome *c*.[23] A subtle increase in ROS caused by partial inhibition of SOD results in apoptosis in isolated cardiac myocytes.[24] Previous studies have demonstrated that apoptosis appears not only in infarcted but also in noninfarcted myocardium after MI.[25] Specifically, apoptosis occurs in the noninfarcted LV late after MI. This is an intriguing observation, in light of the remodeling process known to occur within the noninfarcted area, which is characterized by the loss of myocytes and hypertrophy. In fact, recent studies have suggested cardiac myocyte apoptosis contributes to LV remodeling after MI.[26,27] Importantly, increased oxidative stress occurs concomitantly with increased cardiac myocyte apoptosis within the noninfarcted area. This is a provoking observation, because oxidative stress is a powerful inducer of apoptotic cell death.[28] The present study suggests that the coexistence of oxidative stress and myocyte apoptosis in the noninfarcted LV after MI is causally related. Oxidative stress may mediate myocyte apoptosis, which may lead to myocardial remodeling and failure. Therefore, the decreased mitochondrial oxidative stress due to Prx-3 overexpression could contribute to the amelioration of apoptosis (Figure 5) and eventual post-MI cardiac failure. Second, Prx-3 overexpression prevented the decrease in mtDNA copy number (Figure 6) as well as mitochondrial complex enzyme activities (Table 2). Our previous studies have demonstrated an intimate link between mtDNA damage, increased lipid peroxidation, and a decrease in mitochondrial function, which might play a major role in the development and progression of cardiac failure.[4]

There are several issues to be acknowledged as limitations of this study. First, the differences between WT+MI and TG+MI groups in their echocardiographic measurements are not remarkable, even though they are statistically significant (Table 1). However, our previous study showed that the intraobserver and interobserver variabilities in our echocardiographic measurements for LV dimensions were small, and measurements made in the same animals on separate days were highly reproducible.[12] Therefore, these values are considered to be valid. Second, longer-term follow-up data are not available for the animals in the current study. We therefore could not determine whether the differences between WT+MI and TG+MI groups seen in the present study were more or less significant at later time points, when additional LV remodeling would have been expected to occur.

In conclusion, Prx-3 overexpression inhibited the development of LV remodeling and failure after MI, which was associated with an attenuation of myocyte hypertrophy, apoptosis, and interstitial fibrosis. It also ameliorated mitochondrial oxidative stress as well as mtDNA decline and mitochondrial dysfunction in post-MI hearts. Therapies designed to interfere with mitochondrial oxidative stress could be beneficial to prevent heart failure after MI.

## Acknowledgments

This study was supported in part by grants from the Ministry of Education, Science and Culture (No. 12670676, 14370230, 17390223). A portion of this study was conducted at Kyushu University Station for Collaborative Research I and II.

## Disclosures

None.

## References

1. Ide T, Tsutsui H, Kinugawa S, Suematsu N, Hayashidani S, Ichikawa K, Utsumi H, Machida Y, Egashira K, Takeshita A. Direct evidence for increased hydroxyl radicals originating from superoxide in the failing myocardium. *Circ Res*. 2000;86:152–157.
2. Mallat Z, Philip I, Lebret M, Chatel D, Maclouf J, Tedgui A. Elevated levels of 8-iso-prostaglandin F2α in pericardial fluid of patients with heart failure: a potential role for in vivo oxidant stress in ventricular dilatation and progression to heart failure. *Circulation*. 1998;97:1536–1539.

3. Ide T, Tsutsui H, Kinugawa S, Utsumi H, Kang D, Hattori N, Uchida K, Arimura K, Egashira K, Takeshita A. Mitochondrial electron transport complex I is a potential source of oxygen free radicals in the failing myocardium. *Circ Res*. 1999;85:357–363.
4. Ide T, Tsutsui H, Hayashidani S, Kang D, Suematsu N, Nakamura K, Utsumi H, Hamasaki N, Takeshita A. Mitochondrial DNA damage and dysfunction associated with oxidative stress in failing hearts after myocardial infarction. *Circ Res*. 2001;88:529–535.
5. Suematsu N, Tsutsui H, Wen J, Kang D, Ikeuchi M, Ide T, Hayashidani S, Shiomi T, Kubota T, Hamasaki N, Takeshita A. Oxidative stress mediates tumor necrosis factor-α–induced mitochondrial DNA damage and dysfunction in cardiac myocytes. *Circulation*. 2003;107:1418–1423.
6. Bryk R, Griffin P, Nathan C. Peroxynitrite reductase activity of bacterial peroxiredoxins. *Nature*. 2000;407:211–215.
7. Kang SW, Chae HZ, Seo MS, Kim K, Baines IC, Rhee SG. Mammalian peroxiredoxin isoforms can reduce hydrogen peroxide generated in response to growth factors and tumor necrosis factor-α. *J Biol Chem*. 1998;273:6297–6302.
8. Hattori F, Murayama N, Noshita T, Oikawa S. Mitochondrial peroxiredoxin-3 protects hippocampal neurons from excitotoxic injury in vivo. *J Neurochem*. 2003;86:860–868.
9. Sia YT, Lapointe N, Parker TG, Tsoporis JN, Deschepper CF, Calderone A, Pourdjabbar A, Jasmin JF, Sarrazin JF, Liu P, Adam A, Butany J, Rouleau JL. Beneficial effects of long-term use of the antioxidant probucol in heart failure in the rat. *Circulation*. 2002;105:2549–2555.
10. Kinugawa S, Tsutsui H, Hayashidani S, Ide T, Suematsu N, Satoh S, Utsumi H, Takeshita A. Treatment with dimethylthiourea prevents left ventricular remodeling and failure after experimental myocardial infarction in mice: role of oxidative stress. *Circ Res*. 2000;87:392–398.
11. Ho YS, Magnenat JL, Bronson RT, Cao J, Gargano M, Sugawara M, Funk CD. Mice deficient in cellular glutathione peroxidase develop normally and show no increased sensitivity to hyperoxia. *J Biol Chem*. 1997;272:16644–16651.
12. Shiomi T, Tsutsui H, Hayashidani S, Suematsu N, Ikeuchi M, Wen J, Ishibashi M, Kubota T, Egashira K, Takeshita A. Pioglitazone, a peroxisome proliferator–activated receptor-γ agonist, attenuates left ventricular remodeling and failure after experimental myocardial infarction. *Circulation*. 2002;106:3126–3132.
13. Shiomi T, Tsutsui H, Matsusaka H, Murakami K, Hayashidani S, Ikeuchi M, Wen J, Kubota T, Utsumi H, Takeshita A. Overexpression of glutathione peroxidase prevents left ventricular remodeling and failure after myocardial infarction in mice. *Circulation*. 2004;109:544–549.
14. Ide T, Tsutsui H, Ohashi N, Hayashidani S, Suematsu N, Tsuchihashi M, Tamai H, Takeshita A. Greater oxidative stress in healthy young men compared with premenopausal women. *Arterioscler Thromb Vasc Biol*. 2002;22:438–442.
15. Wood ZA, Schroder E, Robin Harris J, Poole LB. Structure, mechanism and regulation of peroxiredoxins. *Trends Biochem Sci*. 2003;28:32–40.
16. Fisher AB, Dodia C, Manevich Y, Chen JW, Feinstein SI. Phospholipid hydroperoxides are substrates for non-selenium glutathione peroxidase. *J Biol Chem*. 1999;274:21326–21334.
17. Watabe S, Hiroi T, Yamamoto Y, Fujioka Y, Hasegawa H, Yago N, Takahashi SY. SP-22 is a thioredoxin-dependent peroxide reductase in mitochondria. *Eur J Biochem*. 1997;249:52–60.
18. Nonn L, Berggren M, Powis G. Increased expression of mitochondrial peroxiredoxin-3 (thioredoxin peroxidase-2) protects cancer cells against hypoxia and drug-induced hydrogen peroxide–dependent apoptosis. *Mol Cancer Res*. 2003;1:682–689.
19. Banmeyer I, Marchand C, Clippe A, Knoops B. Human mitochondrial peroxiredoxin 5 protects from mitochondrial DNA damages induced by hydrogen peroxide. *FEBS Lett*. 2005;579:2327–2333.
20. Chang TS, Cho CS, Park S, Yu S, Kang SW, Rhee SG. Peroxiredoxin III, a mitochondrion-specific peroxidase, regulates apoptotic signaling by mitochondria. *J Biol Chem*. 2004;279:41975–41984.
21. Dhalla AK, Hill MF, Singal PK. Role of oxidative stress in transition of hypertrophy to heart failure. *J Am Coll Cardiol*. 1996;28:506–514.
22. Nakamura R, Egashira K, Machida Y, Hayashidani S, Takeya M, Utsumi H, Tsutsui H, Takeshita A. Probucol attenuates left ventricular dysfunction and remodeling in tachycardia-induced heart failure: roles of oxidative stress and inflammation. *Circulation*. 2002;106:362–367.
23. Petronilli V, Costantini P, Scorrano L, Colonna R, Passamonti S, Bernardi P. The voltage sensor of the mitochondrial permeability transition pore is tuned by the oxidation-reduction state of vicinal thiols: increase of the gating potential by oxidants and its reversal by reducing agents. *J Biol Chem*. 1994;269:16638–16642.
24. Siwik DA, Tzortzis JD, Pimental DR, Chang DL, Pagano PJ, Singh K, Sawyer DB, Colucci WS. Inhibition of copper-zinc superoxide dismutase induces cell growth, hypertrophic phenotype, and apoptosis in neonatal rat cardiac myocytes in vitro. *Circ Res*. 1999;85:147–153.
25. Palojoki E, Saraste A, Eriksson A, Pulkki K, Kallajoki M, Voipio-Pulkki LM, Tikkanen I. Cardiomyocyte apoptosis and ventricular remodeling after myocardial infarction in rats. *Am J Physiol Heart Circ Physiol*. 2001;280:H2726–H2731.
26. Sam F, Sawyer DB, Chang DL, Eberli FR, Ngoy S, Jain M, Amin J, Apstein CS, Colucci WS. Progressive left ventricular remodeling and apoptosis late after myocardial infarction in mouse heart. *Am J Physiol Heart Circ Physiol*. 2000;279:H422–H428.
27. Oskarsson HJ, Coppey L, Weiss RM, Li WG. Antioxidants attenuate myocyte apoptosis in the remote non-infarcted myocardium following large myocardial infarction. *Cardiovasc Res*. 2000;45:679–687.
28. von Harsdorf R, Li PF, Dietz R. Signaling pathways in reactive oxygen species–induced cardiomyocyte apoptosis. *Circulation*. 1999;99:2934–2941.

## CLINICAL PERSPECTIVE

A growing body of evidence suggests that oxidative stress, an excess generation of reactive oxygen species (ROS), plays a major role in the pathogenesis of heart failure. Furthermore, antioxidants have been shown to exert protective and beneficial effects against this process. Recent studies have suggested that mitochondria are the predominant source of ROS in the failing heart, and mitochondrial antioxidants are expected to be the first line of defense against mitochondrial oxidative stress–mediated myocardial injury. The present study demonstrated that overexpression of peroxiredoxin-3 (Prx-3) inhibited cardiac remodeling and failure after myocardial infarction (MI) created by ligation of the left coronary artery in mice. Prx-3 contains a mitochondrial localization sequence, is found exclusively in the mitochondria, and uses mitochondrial thioredoxin (Trx)-2 as the electron donor for its peroxidase activity. It functions not only by removing $H_2O_2$ formed after the superoxide dismutase (SOD)–catalyzed dismutation reaction but also by detoxifying peroxynitrite. Therefore, the great efficiency of Prx-3 as an antioxidant shown in the present study may be attributable to the fact that it is located in the mitochondria and can utilize lipid peroxides as well as $H_2O_2$ for substrates. The present study not only extends previous investigations that used antioxidants but also reveals a major role for mitochondrial oxidative stress in the pathophysiology of postinfarct heart failure. Therapies designed to interfere with mitochondrial oxidative stress by using antioxidant Prx-3 might also beneficial in preventing clinical heart failure.